Development of an on-line diagnosis system for rotor vibration via model-based intelligent inference

Mingsian R. Bai,[a] Ilong Hsiao, Hsuming Tsai, and Chinteng Lin
Department of Mechanical Engineering, Chiao-Tung University, 1001 Ta-Hsueh Road, Hsin-Chu 30050, Taiwan, Republic of China

(Received 22 July 1998; revised 30 September 1999; accepted 2 October 1999)

An on-line fault detection and isolation technique is proposed for the diagnosis of rotating machinery. The architecture of the system consists of a feature generation module and a fault inference module. Lateral vibration data are used for calculating the system features. Both continuous-time and discrete-time parameter estimation algorithms are employed for generating the features. A neural fuzzy network is exploited for intelligent inference of faults based on the extracted features. The proposed method is implemented on a digital signal processor. Experiments carried out for a rotor kit and a centrifugal fan indicate the potential of the proposed techniques in predictive maintenance. © *2000 Acoustical Society of America.* [S0001-4966(00)03201-X]

PACS numbers: 43.40.Le, 43.40.At [CBB]

INTRODUCTION

Process automation has been a trend in mass-production industries worldwide. In process automation, direct contact with the human operators is reduced and automatic means are generally employed to monitor the health of process elements. Early detection and isolation of machine faults has been a key issue of productivity and safety.

Traditionally, fault detection and isolation (FDI) is carried out on a periodic basis to check either the overall level or the band level of vibrations with regard to a certain threshold and alarms are triggered if the limits are exceeded. This class of methods is known as limit checking.[1–3] As a more advanced approach, computer-based expert systems can also be used.[4,5] However, faults are usually detected by these methods at a rather late stage near failure. Motivated by the need for early FDI, this paper proposes an on-line model-based diagnosis technique for rotator vibration. The required model must be identified on the basis of the input–output relationship of the system of interest. These techniques make use of more information than the pure signal-based methods that are based on only the outputs to the system. The advantage of including a model lies in the early detection and isolation of faults and reduced number of sensors. Model-based methods have been utilized for vibration monitoring of cracked beams and rotors from the structure point of view.[6–9] This paper has a slightly different perspective that is aimed primarily at the common rotor faults in the discrete components and the system as a whole.

The general architecture of these methods can be divided into two major steps: (1) generation of features from the monitored signals and (2) inference and isolation of the faults. The dynamic model of the physical system of interest is identified via either a recursive continuous-time algorithm or a discrete-time parameter estimation algorithm.[10] On the basis of extracted features, fault types are determined by using the neural fuzzy intelligent inference algorithms.[11] The architecture of the model-based method is depicted in Fig. 1.

Rotating machines are chosen as the target application to validate the proposed FDI techniques because they represent a large class of industrial machinery. In particular, we use a rotor kit that is capable of producing several kinds of common faults of rotating machinery. Then, we use a centrifugal fan to justify the practicality of the integrated FDI system.

I. RECURSIVE PARAMETER ESTIMATION FOR ROTORS

A. Continuous-time parameter estimation

Model-based diagnosis algorithms generally fall into two categories: the state estimation methods[1,12] and the parameter estimation methods.[10,13–16] State estimation methods can further be classified into three kinds of schemes: the fault detection filter,[17] the parity space method,[18,19] and the dedicated observer method.[20] In this paper, we choose the parameter estimation method because it reflects more directly the change of system characteristics and is also robust against disturbances and uncertainties.

For processes with lumped parameters that can be linearized about the operating point, the dynamic models usually take the forms of ordinary differential equations

$$y(t)+a_1y^{(1)}(t)+\cdots+a_ny^{(n)}(t) = b_0u(t)+b_1u^{(1)}(t)+\cdots+b_mu^{(m)}(t), \quad (1)$$

with

$$y(t)=Y(t)-Y_0 \text{ and } u(t)=U(t)-U_0, \quad (2)$$

where U_0, Y_0 are the steady-state (or direct current) values of the input signal $U(t)$ and the output signal (t) around the operating point, and $y^{(n)}(t)=d^ny(t)/dt^n$. The process model in Eq. (1) can be written more compactly in a linear regression form

$$y(k)=\psi^T(k)\,\theta(k), \quad (3)$$

with the parameter vector

[a]Electronic mail: msbai@cc.nctu.edu.tw

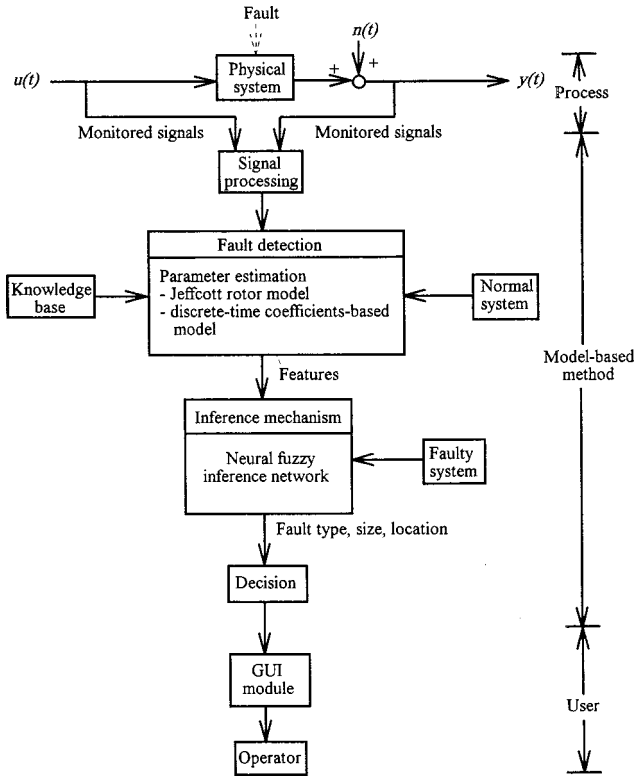

FIG. 1. Architecture of the model-based method for the fault diagnosis system.

$$\theta^T(k)=[a_1\cdots a_n b_0\cdots b_m] \tag{4}$$

and the data vector

$$\psi^T(k)=[-y^{(1)}(t)\cdots-y^{(n)}(t)u(t)\cdots u^{(m)}(t)], \tag{5}$$

where k is the iteration index on the discrete-time base. The task of feature extraction here consists of estimating θ based on the measured ψ. In this paper, the recursive least-square (RLS)[21] algorithm with forgetting factor is utilized to estimate the parameters. Defining the data matrix

$$\psi_k^T=[\psi(1)\psi(2)\psi(3)\cdots\psi(k)], \tag{6}$$

and the covariance matrix

$$\mathbf{P}(k)=[\psi_k^T\psi_k]^{-1}, \tag{7}$$

the procedures are summarized as follows:

(1) Initialize the parameter vector $\hat{\theta}(k=0)$ and the covariance matrix $\mathbf{P}(k=0)=p\mathbf{I}$, with p being a very large constant and $\mathbf{I}$ being the identity matrix.
(2) Obtain the input and output data to form the new data matrix $\psi(k)$ and $y(k)$.
(3) Form the a priori prediction error $\varepsilon(k)$ using

$$\varepsilon(k)=y(k)-\psi^T(k)\hat{\theta}(k-1). \tag{8}$$

(4) Update the parameter estimates $\hat{\theta}(k)$ using

$$\hat{\theta}(k)=\hat{\theta}(k-1)+\mathbf{F}(k)\varepsilon(k), \tag{9}$$

where

$$\mathbf{F}(k)=\frac{\mathbf{P}(k-1)}{\lambda+\psi^T(k)\mathbf{P}(k-1)\psi(k)}\psi(k), \tag{10}$$

and λ is called the forgetting factor that introduces increasing weaker weighting on the old data in the quadratic cost function of $\varepsilon(k)$.[22]

Update the covariance matrix $\mathbf{P}(k)$ using

$$\mathbf{P}(k)=\frac{1}{\lambda}[I-\mathbf{F}(k)\psi^T(k)]\mathbf{P}(k-1). \tag{11}$$

(5) Set $k=k+1$ and go to step (2).

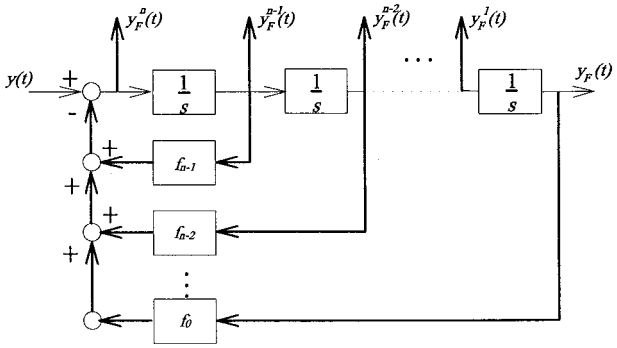

FIG. 2. Block diagram of the state variable filter (SVF).

Some remarks should be made on the practical implementation of the RLS algorithm. In principle, large initial $\mathbf{P}(0)$ (corresponding to large uncertainty and rapid fluctuations) and large forgetting factors λ (close to unity) should be selected if the input signals are not sufficiently persistently exciting or spectrally rich,[22] which is usually the case in the constant-speed operations of rotating machines. Also, proper scaling may be necessary to improve the convergence when some of the model coefficients are out of proportion to the others.

There remains one problem to resolve before the application of the continuous-time parameter estimation. The time derivatives in the data vector ψ are usually unavailable if only the signals $u(t)$ and $y(t)$ are measured. One way to overcome the difficulty is to use the state variable filter (SVF).[23] It is a state representation of an nth-order low-pass transfer function $F(s)$,

$$F(s)=\frac{y_F(s)}{y(s)}=\frac{1}{f_0+f_1 s+\cdots+f_n s^n}, \tag{12}$$

where $y_F(s)$ and $y(s)$ represent the Laplace transform of the filtered output $y_F(t)$ and the original output $y(t)$, respectively. It provides simultaneously the time derivatives (without direct differentiation) and filtering of the noise (Fig. 2). In the paper, we choose a fourth-order Butterworth filter with a cutoff frequency of 200 Hz.

After all the derivatives are obtained from the SVF, the RLS algorithm is employed to calculate the model parameters θ. Assume that the relationship between the model parameters θ and the process coefficients ρ is

$$\theta=f(\rho), \tag{13}$$

or, in matrix form,

$$\theta=\mathbf{C}\mathbf{z}, \tag{14}$$

where $\mathbf{z}$ is a function of ρ, i.e.,

$$\mathbf{z}=g(\rho). \tag{15}$$

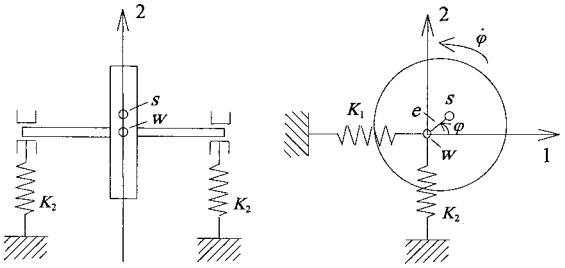

FIG. 3. The Jeffcott rotor model with flexible bearings.

Thus the process coefficients ρ can be obtained from the inverse relationship

$$\rho = f^{-1}(\theta). \tag{16}$$

A useful alternative to the forgoing continuous-time parameter algorithm is the discrete-time parameter estimation algorithm. The discrete-time algorithm follows basically the same line as the continuous-time version, except that the data vector ψ contains the present and past data samples instead of time derivatives. There is no need for the SVF processing in constructing the data. The advantage of the discrete-time algorithm lies in the fact that it accommodates better than the continuous-time version the high-order dynamics of more complicated systems that cannot be modeled as simple rotors.

B. Modeling of rotor dynamics

In the paper, we model the rotor systems in terms of lateral vibrations that reflect the rotor faults commonly encountered in practical applications. A classical rotor model suited for this purpose is the Jeffcott model.[24,25]

The Jeffcott model illustrated in Fig. 3, consists of a massless circular shaft with a fixed rigid circular disc supported by flexible bearings at the center of the shaft. The disc is mounted with its plane perpendicular to the shaft axis. Its mass center S has a radial offset e with the shaft center W. The disc is assumed to move only in the 1-2 plane. The movement of the shaft center W relative to the unloaded position is given by coordinates (y_1, y_2) and the angle of the disc position is given by φ. The position of the point S can be expressed as

$$z_1 = y_1 + e\cos\varphi, \tag{17}$$

$$z_2 = y_2 + e\sin\varphi. \tag{18}$$

Assume that the damping coefficients in directions 1 and 2 are d_1 and d_2, respectively, the stiffness of shaft is K, and two bearings have equal pairs of stiffness K_1 and K_2 in the directions 1 and 2, respectively. The total stiffness of the shaft and bearings is

$$K_1' = \frac{K}{1 + K/2K_1}, \tag{19}$$

$$K_2' = \frac{K}{1 + K/2K_2}. \tag{20}$$

The equations of motion (as functions of y_1, y_2, and φ) can be obtained from applying Newton's second law in translation and rotation.

$$M\ddot{y}_1 + d_1\dot{y}_1 + K_1' y_1 = \mathrm{Me}(\ddot{\varphi}\sin\varphi t + \dot{\varphi}^2\cos\varphi t), \tag{21}$$

$$M\ddot{y}_2 + d_2\dot{y}_2 + K_2' y_2 = \mathrm{Me}(-\ddot{\varphi}\cos\varphi t + \dot{\varphi}^2\sin\varphi t) - G, \tag{22}$$

$$I_p\ddot{\varphi} + e(d_1\dot{y}_1 + K_1' y_1)\sin\varphi t - e(d_2\dot{y}_2 + K_2' y_2)\cos\varphi t = T(t), \tag{23}$$

where M is the mass of the disc, G is the weight of the disc, I_p is the polar moment of inertia of disc, and $T(t)$ is the mechanical torque input. Assuming that y_1 and y_2 are measured with reference to the equilibrium position, we can rewrite Eqs. (21) and (22), adjusted with an angle offset φ_0 that is the angle between the reference point and the center of mass,

$$\ddot{y} + 2\xi_1\omega_{01}\dot{y}_1 + \omega_{01}^2 y_1 = e[\ddot{\varphi}\sin(\varphi + \varphi_0) + \dot{\varphi}^2\cos(\varphi + \varphi_0)], \tag{24}$$

$$\ddot{y}_2 + 2\xi_2\omega_{02}\dot{y}_2 + \omega_{02}^2 y_2 = e[-\ddot{\varphi}\cos(\varphi + \varphi_0) + \dot{\varphi}^2\sin(\varphi + \varphi_0)]. \tag{25}$$

Or,

$$\ddot{y}_1 + 2\xi_1\omega_{01}\dot{y}_1 + \omega_{01}^2 y_1 = e\cos\varphi_0(\ddot{\varphi}\sin\varphi + \dot{\varphi}^2\cos\varphi) + e\sin\varphi_0(\ddot{\varphi}\cos\varphi - \dot{\varphi}^2\sin\varphi), \tag{26}$$

$$\ddot{y}_2 + 2\xi_2\omega_{02}y_2 + \omega_{02}^2 y_2 = e\cos\varphi_0(-\ddot{\varphi}\cos\varphi + \dot{\varphi}^2\sin\varphi) + e\sin\varphi_0(\ddot{\varphi}\sin\varphi + \dot{\varphi}^2\cos\varphi), \tag{27}$$

where

$$\omega_{0i} = \sqrt{\frac{K_i'}{M}}, \tag{28}$$

$$\xi_i = \frac{\sqrt{K_i' M}}{2d_i}. \tag{29}$$

Equations (26) and (27) form the basis of the continuous-time parameter estimation which can be recast into the linear regression forms

$$y_i(k) = \psi_i^T(k)\,\theta_i(k), \quad i = 1,2, \tag{30}$$

where

$$\psi_1^T(k-1) = [\ddot{y}_1\dot{y}_1\ddot{\varphi}\sin\varphi + \dot{\varphi}^2\cos\varphi\ddot{\varphi}\cos\varphi - \dot{\varphi}^2\sin\varphi], \tag{31}$$

$$\psi_2^T(k-1) = [\ddot{y}_2\dot{y}_2\dot{\varphi}^2\sin\varphi - \ddot{\varphi}\cos\varphi\ddot{\varphi}\sin\varphi + \dot{\varphi}^2\cos\varphi], \tag{32}$$

$$\theta_1^T(k) = [-a_{11} - a_{21}b_{11}b_{21}], \tag{33}$$

$$\theta_2^T(k) = [-a_{12} - a_{22}b_{12}b_{22}], \tag{34}$$

and

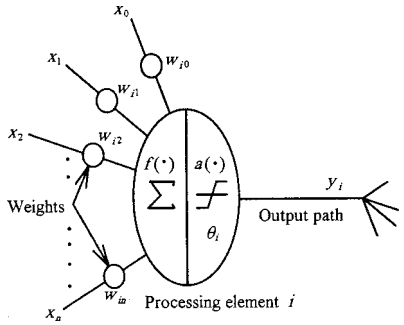

FIG. 4. A schematic diagram of a McCulloch–Pitts neuron (Ref. 26).

$$a_{1i}=1/\omega_{0i}^2, \quad a_{2i}=2\xi_i/\omega_{0i}, \quad b_{11}=b_{12}=e\cos\varphi_0, \quad b_{21}=b_{22}=e\sin\varphi_0. \tag{35}$$

From the model parameters, the process coefficients can be recovered as

$$\omega_{0i}=\frac{1}{\sqrt{a_{1i}}}, \quad i=1,2, \tag{36}$$

$$\xi_i=\frac{a_{2i}}{2\sqrt{a_{1i}}}, \quad i=1,2, \tag{37}$$

$$e=\sqrt{b_{11}^2+b_{21}^2}=\sqrt{b_{12}^2+b_{22}^2}. \tag{38}$$

II. INTELLIGENT INFERENCE ALGORITHMS FOR FDI

In the paper, artificial neural network and fuzzy theory are utilized for inference of rotor faults. Figure 4 shows a mathematical model of the biological neuron, usually called an M-P neuron,[26,27] where the ith processing element computes a weighted sum of its inputs $x_0, x_1, x_2, \ldots, x_n$ and outputs $y_i=1$ (firing) or 0 (not firing) according to whether this weighted input sum is above or below a certain threshold θ_i,

$$y_i(k+1)=a(f)\sum_{j=0}^{n} w_{ij}x_i(k)-\theta_i, \tag{39}$$

where k is the iteration index of input and output and the activation function $a(f)$ is a unit step function,

$$a(f)=\begin{cases}1, & \text{if } f\geqslant 0\\ 0, & \text{otherwise}\end{cases}. \tag{40}$$

In the paper, the supervised learning network with back-propagation is employed. The algorithm generally includes two phases: the learning (training) process and the recall process. In the supervised learning, the objective is to reduce the error between the desired output and the calculated output. To quantify the quality of learning, an error function is utilized,

$$E=\frac{1}{2}\sum_i (T_i-A_i)^2, \tag{41}$$

where T_i is the desired output vector and A_i is the calculated output vector. Methods such as the gradient search algorithm can be used for finding the minimum of E. In the training phase, the network weightings are updated according to the sensitivity of the error function with respect to the weightings

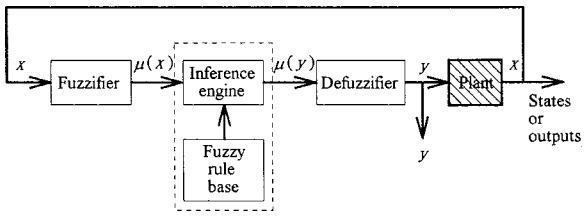

FIG. 5. Block diagram of a fuzzy logic controller (FLC) (Ref. 26).

$$\Delta w_{ij}^n=-\eta\frac{\partial E}{\partial w_{ij}^n}, \tag{42}$$

where Δw_{ij}^n is the increment of the weighting between the ith processing element of the $(n-1)$th layer and the jth processing element of the nth layer, and η is the step size for the gradient search algorithm.

Since Zadeh introduced in 1965 the fuzzy sets to represent vagueness of linguistics, a rapid growth in the use of fuzzy theories is witnessed in many scientific applications.[26] In contrast to classical sets that are crisp sets based on the binary logic (''Truth'' or ''False''), the fuzzy sets are not only to classify one element belonging to a set or not, but to fuzzify in ''Truth'' with some degree of membership. Let $\tilde{A}$ be a fuzzy set and U be its universe of discourse

$$\tilde{A}=\{(x,\mu_{\tilde{A}}(x))|x\in U\}, \tag{43}$$

where $\mu_{\tilde{A}}(x)$ is the membership function of x in the fuzzy set $\tilde{A}$ that represents the degree of x belonging to the fuzzy set $\tilde{A}$, and its value is usually in the interval [0, 1]. A general architecture of a fuzzy logic control (FLC) system including a fuzzifier, a fuzzy rule base, an inference engine, and a defuzzifier, is shown in Fig. 5. If the output from the defuzzifier is not a control action (as in our case) for a plant, the system becomes a fuzzy logic decision system.

In this study, a Self-cOnstructing Neural Fuzzy Inference Network (SONFIN), which is inherently a fuzzy rule-based model possessing neural network,[26] is employed for intelligent inference and isolation of faults. This technique integrates the advantages of both artificial neural network and the fuzzy theory, and is well suited for automatic inference required in the FDI application. The structure of the SONFIN is shown in Fig. 6, whereby the network consists of six layers: the input layer, the membership layer, the fuzzy rule layer, the normalization layer, the consequent layer, and the output layer. The network realizes the following fuzzy model:

$$\text{Rule } i\text{: IF } (x_1 \text{ is } A_{i1} \text{ and}\cdots\text{and } x_n \text{ is } A_{in})$$
$$\text{THEN } (y \text{ is } m_{0i}+a_{ji}x_j+\cdots), \tag{44}$$

where A_{ij} is a fuzzy set, m_{0i} is the center of a symmetric membership function on y, and a_{ji} is a consequent parameter. There are no rules initially, but they are created and adapted as on-line learning proceeds via simultaneous structure and parameter identification. The learning process involves four steps: input/output space partitioning, construc-

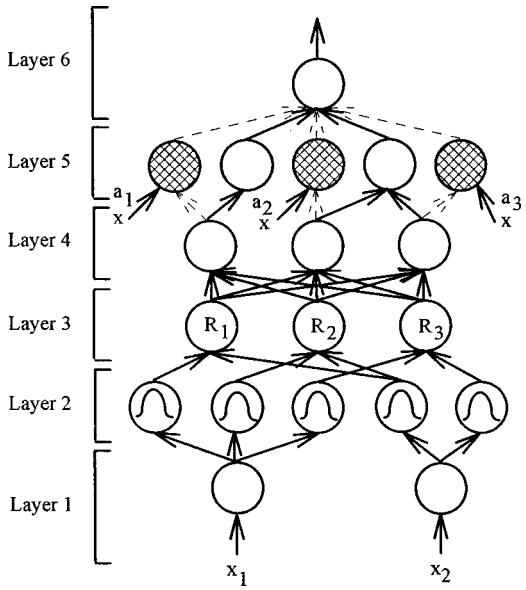

FIG. 6. Structure of the Self cOnstructing Neural Fuzzy Inference Network (SONFIN). In the figure, *x*'s are input variables; *R*'s are fuzzy rules; *a*'s are weightings in back-propagation.

tion of fuzzy rules, optimal consequent structure identification, and parameter identification. The first three steps are for structure learning and the last step for parameter learning. In the structure identification of the precondition part, the input space is partitioned by using an aligned clustering-based algorithm, while in the structure identification of the consequent part only a single value selected by a clustering method is assigned to each rule initially. Afterwards, some additional significant input variables selected via the Gram–Schmidt orthogonalization for each rule will be added to the consequent part incrementally. Furthermore, to enhance the knowledge representation, a linear transformation for each input variable is incorporated into the network so that fewer rules are needed. Finally, in parameter identification, the RLS algorithm is used to tune the parameters in layer 5 and the back-propagation algorithm is used to update the parameters of the membership functions in layer 2. The trained neural fuzzy network is used for the subsequent inference for faults. The unique features of SONFIN are twofold. First, the structure and the weights of the network are automatically adjusted. Second, a high-dimensional fuzzy system is implemented with a small number of rules and fuzzy terms. Due to the physical meaning of the fuzzy if–then rule, each input node in the SONFIN is only connected to its related rule nodes through its term nodes, instead of being connected to all the rule nodes in layer 3. This results in a small number of weights to be tuned. In some cases, however, it is time consuming to train the network provided the number of inputs is large. To alleviate the difficulty, a Discriminatory Information (DI) method[4] can be

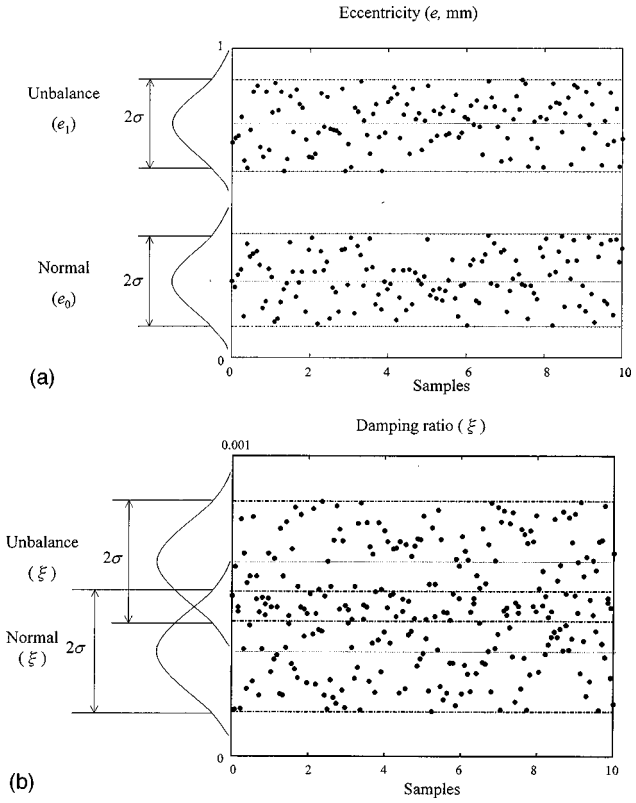

FIG. 7. Schematic of the discriminatory information (DI) method. (a) A more discriminatory feature; (b) a less discriminatory feature.

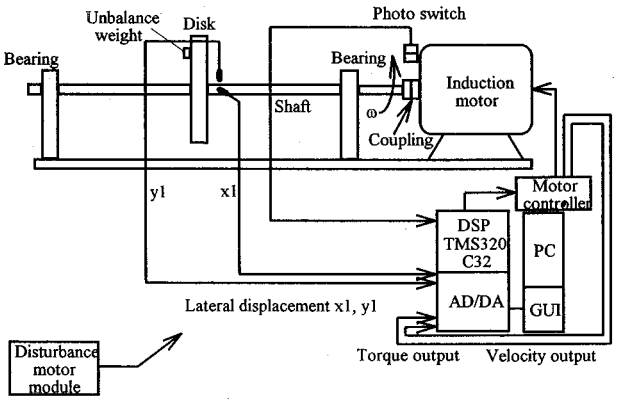

FIG. 8. Experimental arrangement of the rotor kit.

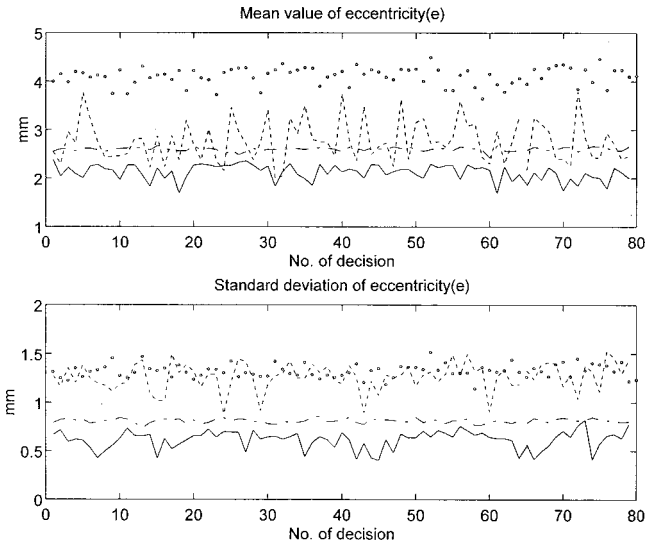

FIG. 9. The time variation of *e* in the normal, imbalanced, looseness, and faulty bearing conditions of the rotor kit. Normal: ——, imbalanced: · · , looseness: –·–, and faulty bearing: --.

TABLE I. Effects of different faults on the estimated continuous-time process coefficients for the rotor kit. ($\overline{x}$: average; σ: standard deviation; +: increase; −: decrease; *: insignificant).

	Parameters									
Condition	$\overline{x}$ of ω_{01}	$\overline{x}$ of ω_{02}	$\overline{x}$ of ξ_1	$\overline{x}$ of ξ_2	$\overline{x}$ of e	σ of ω_{01}	σ of ω_{02}	σ of ξ_1	σ of ξ_2	σ of e
Disturbance	−	−	*	+	*	+	+	+	+	+
Imbalance	+	*	−	*	+	+	*	−	*	+
Misalignment	+	+	+	+	+	+	+	+	+	+
Looseness	*	−	−	−	−	*	*	−	−	−
Faulty bearing	−	*	+	*	*	+	*	+	*	+

used to calculate the statistics of the data and retain only the inputs that account for the distinct features associated with the different conditions. The basic idea of the DI method is to choose the features that have distributions of distinct means and small spreads with respect to different conditions. The procedure is summarized as follows:

(a) A test is performed to collect 128 samples of system parameters, e.g., eccentricity, damping ratio, natural frequency, etc.
(b) Probability density functions (pdf) are calculated for the extracted parameters in an off-line manner.
(c) If the mean value deviates from the normal case by 20% and the ''2-σ'' regions do not overlap, then the parameter is considered a good discriminator for the fault type of interest and thus serves as an input variable to the network. Otherwise, the parameter is discarded.

An example of the use of the DI method is shown in Fig. 7. The feature of Fig. 7(a) shows more isolated mean values and smaller variances than that of Fig. 7(b). Thus the former feature is preferably used as the principal input to the network.

III. EXPERIMENTAL INVESTIGATIONS

Experiments were carried out to validate the proposed FDI technique. In particular, we verified the feature generation and fault inference algorithm by using a rotor kit that is capable of producing common rotor faults. Then, a centrifugal fan was also used to justify the practicality of the FDI system.

A. Rotor kit

A rotor kit is used in the first part of the experiments (Fig. 8). The rotor kit consists of a constant-speed (1500 rpm) induction motor, a coupling, a steel shaft, two ball-bearing supports, an aluminum disk, and a disturbance motor module. Five common rotor faults, imbalance, misalignment, disturbance, mechanical looseness, and faulty bearings can be conveniently produced by the rotor kit. Imbalance is created by adding an imbalanced weight on the disk. Misalignment is created by dislocating the coupling with a radial offset. Disturbance is created by a frictional disk driven by another induction motor running at a different angular frequency. The mechanical looseness is created by loosening one of the four bolts at the two bearing supports. The bearing fault is created by using a damaged outer ring. On the other hand, the FDI system consists of two eddy-current probes, a photo switch (for angular frequency measurement), and a personal computer equipped with a DSP card (TMS320C32) and 32 analog I/O channels.

In case 1, the FDI method based on continuous-time parameter estimation is investigated. Lateral displacements in both horizontal and vertical directions near the center of the disc are measured by two eddy-current probes. The angular velocity Ω is measured by a photo switch. The measured signals are fed to the DSP via the analog I/O module with a sampling rate 200 Hz. Using the SVF method, the time derivatives of displacements are calculated. Based on the data, the continuous-time RLS algorithm is employed to generate the features including five process coefficients. The DI procedure is used to preprocess the features and remove the insignificant inputs. These data features then become the input vector to the neural fuzzy network. In the first (training) stage of 12-sec measurement, five types of fault and the normal condition are produced by the rotor kit, and the data features are calculated to train the neural fuzzy network. In the second (recall) stage, the rotor is restarted for five times and for each time the faults are regenerated to verify the trained network. Each time record is further divided into ten sets to represent ten experiments. There are altogether $6\times5\times10=300$ experiments. Figure 9 shows the variations of e in the normal, imbalanced, mechanical looseness, and faulty bearing conditions, respectively, of the rotor kit. The variations of the other process coefficients in the other conditions during an ongoing experiment are similarly calculated. The effects of five types of fault on the estimated process coefficients for the rotor kit are summarized in Table I. Appar-

TABLE II. Performance of the continuous-time model-based FDI technique for the rotor kit.

	Condition					
Result	Normal	Disturbance	Imbalance	Misalignment	Looseness	Faulty bearing
Normal	100%	0%	0%	0%	0%	0%
Disturbance	0%	92%	0%	0%	0%	0%
Imbalance	0%	8%	100%	0%	0%	0%
Misalignment	0%	0%	0%	100%	2%	0%
Looseness	0%	0%	0%	0%	98%	8%
Faulty bearing	0%	0%	0%	0%	0%	92%
Average rate of correct inference: 97.0%						

TABLE III. Performance of the discrete-time model-based FDI technique model for the rotor kit.

Result	Condition					
	Normal	Disturbance	Imbalance	Misalignment	Looseness	Faulty bearing
Normal	100%	0%	0%	0%	0%	0%
Disturbance	0%	100%	0%	0%	0%	0%
Imbalance	0%	0%	98%	0%	0%	0%
Misalignment	0%	0%	0%	96%	0%	0%
Looseness	0%	0%	2%	4%	100%	0%
Faulty bearing	0%	0%	0%	0%	0%	100%
Average rate of correct inference: 99.0%						

ently, it is very difficult for an experienced operator to detect and isolate the fault by merely looking at the trends in the table. This calls for the capability of automatic machine-learning of the neural fuzzy network. Table II summarizes the performance of the continuous-time FDI technique with neural fuzzy inference for the rotor kit. The result appears acceptable (average rate of correct inference $=97\%$).

In case 2, the FDI technique based on discrete-time parameter estimation is examined. The foregoing assumption that the angular frequency is constant is relaxed. It is assumed that the discrete-time model of the rotor system is of the form

$$\begin{aligned} y_1(k) = & -a_{1i}y_1(k-1) - a_{2i}y_1(k-2) \\ & + b_{1i}\dot{\omega}\cos(\omega k) + b_{2i}\dot{\omega}\cos(\omega(k-1)) \\ & + b_{3i}\dot{\omega}\sin(\omega k) + b_{4i}\dot{\omega}\sin(\omega(k-1)), \\ & i = 1,2, \end{aligned} \tag{45}$$

where a's and b's are model parameters to be determined and $\dot{\omega}$ is the time derivative of ω that is calculated by the SVF. The above equations can be cast into the linear regression form $y(k) = \psi^T(k)\theta(k)$ with the data vectors

$$\begin{aligned} \mathbf{\Psi}_i^T(k-1) = & [y_i(k-1)y_i(k-2)\dot{\omega}\cos(\omega k)\dot{\omega} \\ & \times \cos(\omega(k-1))\dot{\omega}\sin(\omega k) \\ & \times \dot{\omega}\sin(\omega(k-1))], \quad i = 1,2, \end{aligned} \tag{46}$$

and the parameter vectors

$$\theta_i^T(k) = [-a_{1i} - a_{2i} b_{1i} b_{2i} b_{3i} b_{4i}]. \tag{47}$$

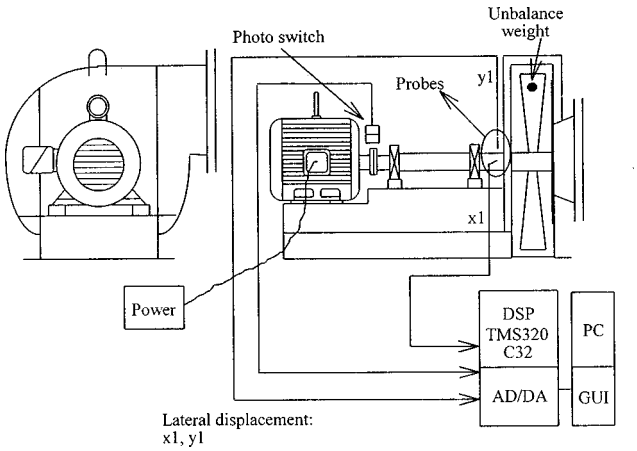

FIG. 10. Experimental arrangement of the centrifugal fan.

Other than the parameter estimation model, the experimental setup remains the same as in the continuous-time case. The discrete-time parameter estimation algorithm is employed to generate the features that in turn become the input vectors to the neural fuzzy inference network. Following a procedure similar to the continuous-time algorithm, the neural fuzzy network is necessary to infer the fault types, based on the features (model parameters in this case) extracted earlier by the discrete-time RLS algorithm. Table III summarizes the performance of the discrete-time FDI technique with neural fuzzy inference for the rotor kit. In comparison with the continuous-time method, the result appears to be slightly improved (average rate of correct inference $=99.0\%$).

B. Centrifugal fan

A more practical system, a two-horsepower centrifugal fan, is chosen for validating the proposed FDI technique. The experimental setup including the fan and the FDI system is shown in Fig. 10. The fan system consists of a constant-speed (1750 rpm) AC induction motor, a steel shaft, a coupling, two bearing supports, and 12 impellers. Four common faults of centrifugal fans, including imbalance, misalignment, mechanical looseness, and faulty bearing are investi-

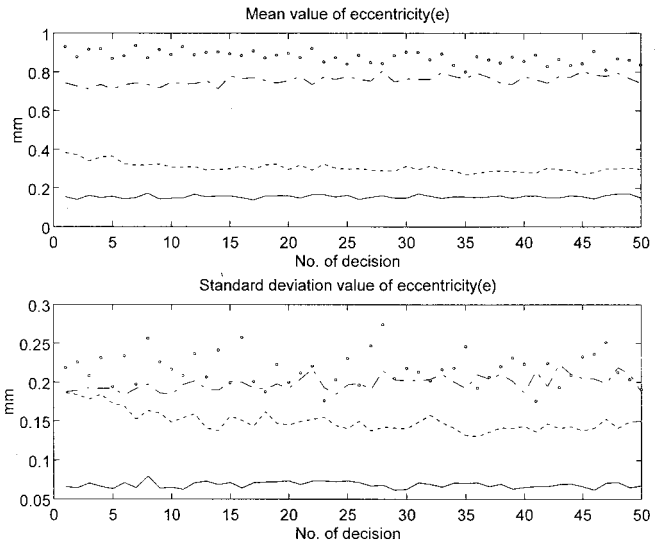

FIG. 11. The time variation of e in the normal, imbalanced, looseness, and faulty bearing conditions of the centrifugal fan. Normal: ——, imbalanced: · ·, looseness: –·–, and faulty bearing: --.

TABLE IV. Performance of the continuous-time model-based FDI technique for the centrifugal fan.

Result	Condition				
	Normal	Imbalance	Misalignment	Looseness	Faulty bearing
Normal	92%	0%	0%	0%	0%
Imbalance	0%	100%	0%	0%	0%
Misalignment	0%	0%	100%	0%	0%
Looseness	8%	0%	0%	100%	0%
Faulty bearing	0%	0%	0%	0%	100%
Average rate of correct inference: 98.4%					

gated in the experiment. The faults are created the same way as the earlier procedures in rotor kit, except that the faulty bearing was replaced with a lubricated bearing.

In case 1, the FDI technique based on continuous-time parameter estimation is examined. Lateral displacements in both horizontal and vertical directions near the impellers are measured by two eddy-current probes. The angular velocity Ω is measured by the photo switch. The other conditions are the same as in case 1 of the rotor kit. Following a procedure similar to the continuous-time algorithm, the neural fuzzy network is necessary to infer the fault types, based on the features extracted earlier by the RLS algorithm. Figure 11 shows the variations of e in the normal, imbalanced, mechanical looseness, and faulty bearing conditions, respectively. The neural fuzzy network is used to infer the fault types, based on the features (process coefficients in this case) extracted earlier by the continuous-time RLS algorithm. Table IV summarizes the performance of the continuous-time FDI technique with neural fuzzy inference for the centrifugal fan. The result appears acceptable (average rate of correct inference$=98.4\%$).

In case 2, the FDI method based on the discrete-time parameter estimation technique is examined. The foregoing assumption that the angular frequency is constant is relaxed. The other conditions remain unchanged from case 2 of the rotor kit. Following a procedure similar to the continuous-time algorithm, the neural fuzzy network is necessary to infer the fault types, based on the features extracted earlier by the RLS algorithm. Table V summarizes the performance of the discrete-time FDI technique with neural fuzzy inference for the centrifugal fan. Compared to the continuous-time method, the result appears excellent (average rate of correct inference$=100.0\%$). It is noted from Tables II–V that the ''false alarm'' rates and ''failure-to-alarm'' rates are all zero except the case of the centrifugal fan, where 8% of the data under ''normal'' conditions are misinterpreted as looseness faults. In these experiments, 97% detection rate is considered sufficient.

TABLE V. Performance of the discrete-time model-based FDI technique for the centrifugal fan.

Result	Condition				
	Normal	Imbalance	Misalignment	Looseness	Faulty bearing
Normal	100%	0%	0%	0%	0%
Imbalance	0%	100%	0%	0%	0%
Misalignment	0%	0%	100%	0%	0%
Looseness	0%	0%	0%	100%	0%
Faulty bearing	0%	0%	0%	0%	100%
Average rate of correct inference: 100.0%					

IV. CONCLUDING REMARKS

An on-line FDI system for rotator vibration is presented. The development of the proposed methods is divided into two stages. First, data features are generated based on two model-based methods. Second, fault types are determined based on the extracted features via neural fuzzy inference algorithms. The proposed FDI system is implemented on a DSP. The usefulness of the proposed technique in identifying common rotor faults has been justified by experiments conducted for a rotor kit and a centrifugal fan. From the experimental results, the discrete-time parameter estimation approach that does not require analytical modeling of the system yields better performance than the continuous-time approach. However, the success of the methods hinges on the proper choices of the model structures.

The proposed FDI technique can readily be extended to other systems such as centrifugal pumps, centrifugal compressors, and machine tools. The system will be extended for handling multiple faults. In practical applications, information is generally incomplete. The machine condition is generally unknown so that the field data are insufficient for reliable training of the network. Thus enhancing the present neural fuzzy inference network, in light of machine learning and human knowledge, for an expert system suited for robust FDI will be the focus of future research.

ACKNOWLEDGMENTS

Special thanks go to Dr. G. H. Chen for the helpful discussions on the FDI subject. The work was supported by the Institute of Occupational Safety and Health (IOSH), Council of Labor Affairs, Executive Yuan in Taiwan, Republic of China, under the project ''Development of Hazard-Preventive Techniques of Major Hydraulic Machinery.''

[1] P. M. Frank, ''Fault diagnosis in dynamic systems using analytical and knowledge-based redundancy—A survey and some new results,'' Automatica **26**, No. 3, 459–474 (1990).
[2] S. J. Mitchell, *Machinery Analysis and Monitoring* (Penn Well, Oklahoma, 1981).
[3] J. E. Berry, ''Proven method for specifying both spectral alarm bands as well as narrowband alarm envelopes using today's predictive maintenance software system,'' BandAid Technical Literature, Technical Associates of Charlotte, Inc., Charlotte, NC, 1993.
[4] S. Braun, *Mechanical Signature Analysis—Theory and Applications* (Academic, Orlando, Florida, 1986).
[5] H. Kumamoto, ''Application of expert system techniques to fault diagnosis,'' Chem. Eng. J. **29**, 1–9 (1984).
[6] R. L. Actis and A. D. Dimarogonas, ''Non-linear effects due to closing cracks in vibrating beams,'' ASME Des. Eng. Div. Publ. DE Struct. Vib. Acoust. **18**, 99–104 (1989).
[7] J. Wauer, ''On the dynamics of cracked rotors: A literature survey,'' Appl. Mech. Rev. **43**, 13–17 (1990).
[8] X. T. C. Man, L. M. McClure, Z. Wang, and R. D. Finch, ''Slot depth resolution in vibration signature monitoring of beams using frequency shift,'' J. Acoust. Soc. Am. **95**, 2029–2037 (1994).
[9] X. T. C. Man and R. D. Finch, ''Vibration monitoring of slotted beams using an analytical model,'' J. Acoust. Soc. Am. **102**, 382–390 (1997).

[10] R. Isermann, ''Fault diagnosis of machines via parameter estimation and knowledge processing—tutorial paper,'' Automatica **29**, No. 4, 815–835 (1993).
[11] C. F. Juang and C. T. Lin, ''An on-line self-constructing neural fuzzy inference network and its applications,'' IEEE Trans. Fuzzy Systems **6**, No. 1,12–13 (1998).
[12] P. M. Frank, ''Analytical and qualitative model-based fault diagnosis—A survey and some new results,'' European J. Control **2**, 6–28 (1996).
[13] R. Isermann, ''Process fault detection based on modeling and estimation methods—A survey,'' Automatica **20**, No. 4, 387–404 (1984).
[14] R. Isermann, ''Process fault diagnosis based on process model knowledge—Part I. Principles for fault diagnosis with parameter estimation,'' J. Dyn. Syst., Meas., Control **113**, No. DEC, 620–626 (1991).
[15] R. Isermann, ''Process fault diagnosis based on process model knowledge—Part II: Principles for fault diagnosis with parameter estimation,'' J. Dyn. Syst., Meas., Control **113**, No. DEC, 627–633 (1991).
[16] R. Isermann, ''Estimation of physical parameters for dynamic processes with application to an industrial robot,'' Int. J. Control **55**, No. 6, 1287–1298 (1992).
[17] K. L. Jones, ''Failure detection in linear systems,'' The Charles Stark Draper Laboratory, Cambridge, MA, Rep. T-608.
[18] E. Y. Chow and A. S. Willsky, ''Analytical redundancy and the design of robust failure detection systems,'' IEEE Trans. Autom. Control. **AC-29**, No. 7, 603–614 (1984).
[19] J. Gertler, ''Residual generation in model-based fault diagnosis,'' Control Theory Advanced Technology **9**, No. 1, 259–285 (1993).
[20] R. J. Patton and J. Chen, ''Robust fault detection of jet engine sensor systems using eigenstructure assignment,'' J. Guid. Control. Dyn. **15**, No. 6, 1491–1497 (1992).
[21] L. Ljung, *System Identification: Theory for the User* (Prentice-Hall, Englewood Cliffs, NJ, 1987).
[22] G. C. Goodwin and K. S. Sin, *Adaptive Filtering Prediction and Control* (Prentice-Hall, Englewood Cliffs, NJ, 1984).
[23] P. C. Young, ''Parameter estimation for continuous-time models—A survey,'' Automatica **17**, 23–39 (1981).
[24] *Handbook of Rotordynamics*, edited by E. F. Ehrich (McGraw-Hill, New Delhi, India, 1992).
[25] K. Erwin, *Dynamics of Rotors and Foundations* (Springer-Verlag, Berlin, 1993).
[26] C. T. Lin and Lee C. S. George, *Neural Fuzzy Systems* (Prentice-Hall, Englewood Cliffs, NJ, 1996).
[27] T. Kohonen, ''An introduction to neural computing,'' Neural Networks **1**, 3–16 (1988).